

SYNTHESIS REPORT

NON-CONFIDENTIAL / UNCLASSIFIED

CONTRACT NO.: BREU-0422

PROJECT NO.: BE-4515

TITLE: Economic and Reliable Turbine Blading by Low Cost Single Crystal Alloy, Casting Process and Non-Destructive Testing

PROJECT COORDINATOR: MTU (D)

PARTNERS: ONERA (F)
THYSSEN GUSS AG (D)
PRECICAST SA (CH)
TURBOMECA (F)
SULZER BROTHERS LIMITED (CH)

REFERENCE PERIOD FROM (d m y) to (d m y) 01/08/91 to 30/06/95

STARTING DATE: 1. AUGUST 1991 DURATION: 47 MONTHS



PROJECT FUNDED BY THE EUROPEAN COMMUNITY UNDER THE BRITE/EURAM PROGRAMME

DATE: 12 OCTOBER 1995

0 **Title, authors' names and addresses**

Economic and Reliable Turbine Blading by Low Cost Single Crystal Alloy, Casting Process and Non-Destructive Testing

Dr. Khan, Dr. Caron	ONERA 29 AV de la Division Leclerc F-92322 Chatillon Cedex
Dr. Dormer	THYSSEN GUSS AG Bressemerstr. 80 D-44725 Bochmann
Mr. Guido	PRECICAST SA Via Resigna CH-6883 Novazzano
Mr. Guazzone, Mr. Fournier	TURBOMECA F-6451 1 Fordes Cedex
Dr. Wortmann, Mr. Buchmann	MTU Dachauer Str. 665 D-80976 München
Mr. Rossmann	SULZER BROTHERS LIMITED CH-8404 Winterthur

1 **Abstract**

The project reported pursued various but, nevertheless, complementary objectives aiming at reducing the cost of DS and SC technology:

i) to test the influence of small modifications of chemistry on the creep behaviour of the MC2 alloy in order to optimize the alloy composition in respect of the creep strength, ii) to develop a modified version of the MC2 alloy with improved high-temperature oxidation resistance, iii) to demonstrate the suitability of the SMCT process for the solidification of components in a production environment, iv) to improve existing modelling tools for this process and v) to further develop the CRYSTAL system for NDT purposes.

The various objectives have been achieved, however to varying degrees.

2 **Introduction**

After more than 20 years of development, single-crystal alloys were successfully introduced in turbine engines. The situation now is characterized by a rapidly growing demand for single-crystal components for high performance engines due to their unique potential for a combination of different properties: High temperature stability, creep, and thermal fatigue strength,

yield and tensile strength, as well as good oxidation resistance. These single-crystal (SC) alloys will be applicable to various types of components for high-temperature service. The first generation of these alloys are derivatives of alloys previously used as equiaxed or directionally solidified (DS) materials primarily by omitting grain boundary strengthening elements. Single-crystal technology has proved to be reliable in view of the stringent aeronautical requirements. The availability of this class of components became an essential for competitive engines. However, accumulated in-service experience has led to the identification of some handicaps:

One essential handicap of single crystal technology is high cost, caused by

- alloy constitution, e.g. elements like rhenium in some high performance single crystal alloys developed in the USA
- casting process which requires capital investment for furnaces dedicated to SC and DS production only
- high proportion of NDT cost to assess specific SC quality features

The approach of the project therefore was to significantly reduce cost in each respective field.

3 Technical description and results

3.1 Alloy development

3.1.1 Introduction

The high strength nickel base superalloy MC2 was designed for single crystal turbine blade and vane applications [1]. The main objective was to define an alloy with a simple chemical composition, without expensive or heavy elements such as rhenium frequently used in the second generation single crystal superalloys such as CMSX-4 [2], while showing a comparable creep strength at high temperatures. This objective was attained with MC2 which offers a creep temperature advantage of more than 40°C over the first generation single crystal superalloy.

The objectives of the present work were: i) to test the influence of small modifications of chemistry on the creep behaviour of the MC2 alloy in order to optimize the alloy composition in respect of the creep strength, ii) to develop a modified version of the MC2 alloy with improved high temperature oxidation resistance.

3.1.2 Creep strength

Five alloys derived from MC2 (Table 1) were cast as <001> single crystal bars by the withdrawal process using a temperature gradient of 40 °C.cm⁻¹ and a withdrawal rate of 10 cm. h⁻¹. The as-cast alloys contained various amounts (0 to 1.8%) of γ/γ' eutectic pools in the interdendritic areas, which

were totally eliminated by applying a solution heat treatment for 3 hours at a temperature within the 1290-1320°C range, depending on the alloy chemistry. A subsequent two-step precipitation heat treatment, 1100°C/4 hrs/A.C., produced a homogeneous distribution of cuboidal precipitates with a mean size close to 0.4 µm.

The tensile creep properties of the single crystal alloys in the 850-1100°C temperature range are compared in Table II to data obtained on MC2. Analysis of the results showed that the decrease of the level of the γ' forming elements Al and Ti (alloy EX 51) caused a drop in stress-rupture strength only at 1000 and 1050°C, whereas the decrease of the W content (alloy FC 38) reduced the creep rupture lives in the whole 850-1050°C temperature range. The elimination of Co together with the reduction of the Cr concentration (alloy FY 88) lowered the high temperature creep strength in the 760-1100°C temperature range. At the highest temperatures (1050-1100°C), a high Mo/W ratio (alloy FZ 88) seems to be more favorable for the creep strength. Whereas, the creep lives are longer at low and intermediate temperature (760-950°C) when the Mo/Ni ratio is reduced (alloy FZ 91).

The overall results on the experimental alloys show that the composition of the original MC2 alloy must be kept unchanged and carefully controlled in order to maintain the material's high level of creep strength,

3.1.3 Oxidation resistance

Previous studies conducted at ONERA on the single crystal superalloy AM I and AM3 have shown that their oxidation resistance in air at 1100°C can be dramatically improved by small additions of silicon and hafnium [3]. Such chemistry modification was tested on MC2 in order to verify if a similar improvement could be obtained for this alloy.

Two MC2 heats were melted in a high vacuum induction furnace with dopings of Si and Hf in order to obtain respective contents of 1000 ppm. Chemical analyses of samples of the two heats revealed respective Si levels of 0.10 and 0.09wt% and Hf concentrations of 0.11 and 0.09wt.% <001>. Single crystal bars were cast from these heats using the withdrawal process.

Additions of Si and Hf increased the volume fraction of γ/γ' eutectic pools from 0.3 to 1.6% in the as-cast MC2 single crystals. The γ' -solution heat treatment window of MC2 is 1290 -1320°C. It was reduced in the modified alloy where incipient melting occurred at 1310°C and solutionizing of the γ/γ' pools was not totally completed after a 3-hour hold at 1290°C. Nevertheless, a heat treatment at 1295°C for 3 hours was sufficient to eliminate the largest part of the eutectic pools and the totality of the secondary γ' precipitates.

Constant load stress-rupture tests were conducted in the 760-1050°C temperature range on fully heat-treated (1295°C/3 hrs/A.C. + 1100°C/4 hrs/A.C.

+ 850 °C/24 hrs/A. C.) single crystal bars of MC2 + Si + Hf. The creep strength of the modified MC2 alloy appeared slightly lower than that of MC2 alloy at 760, 950 and 1010°C, and comparable at 1050°C (Table II).

The cyclic oxidation resistance in static air at 1100°C of the MC2 modified alloy was dramatically improved compared to that of the base alloy (fig. 1). After 400 cycles, the surface of the MC2 sample showed severe degradation, whereas the surface of the modified alloy sample was practically not affected even after 1000 cycles. Sectioning of the MC2 modified sample exhibited a thin, dense and continuous external alumina (Al_2O_3) protective layer, whereas the MC2 sample showed an irregular superficial layer of complex oxide with extended internal oxides [3]. Close examination of the oxide scale on the MC2 modified sample revealed the existence of Al_2O_3 pegs initiated by Hf-rich oxides and growing from the oxide metal interface. A survey of the literature showed that the improvement in high temperature oxidation resistance of superalloys by addition of hafnium can be explained by a keying effect of the Al_2O_3 scale by pegs initiated on Hf-rich oxides [4, 5], as observed in the MC2 modified alloy. These observations showed that the additions of Si and Hf improve the adherence of the external protective Al_2O_3 scale, thus preventing spallation and formation of less protective oxides.

3.1.4 Alloy castability

Introduction

Castability of MC2 single crystal bars and blades was evaluated by using two different casting processes: i) the SVW (small volume withdrawal) process used by THYSSEN, ii) the SMCT (Sulzer MTU Casting Technology) process used by PRECICAST.

3.1.4.1 SVW Process

The MC2 master melt was produced by Aubert & Duval (Heat VM 1913) (Table I). Casting trials were performed using shell moulds with 8 cylindrical rods each with a diameter of 16 mm. After solution treatment at 1300°C, no grain structure defects, especially no recrystallization, were detected. These casting trials showed that MC2 has a castability comparable to that of CMSX-6, a competitive alloy which is currently produced using the SVW process. Microstructural assessment and chemical analyses performed on an as-cast single crystal bar showed good chemical and microstructural homogeneities all along the bar. The dendrite size (~280 µm) and the fraction of γ/γ' eutectic pools (~0.9%) were fairly constant along the bar.

3.1.4.2 SMCT Process

Precicast cast MC2 single crystal bars and ARRIUS2C blades in their conventional vacuum furnace using the SMCT process. This process is a directional solidification process with employs "mold integrated heat flow control" to create the required unidirectional heat flow at the solidification front,

instead of the usual withdrawal process. From the casting technique no particular difficulty was found and the behaviour of MC2 during melting, casting and cooling was similar to that of other competitive single crystal alloys already used at PRECICAST (CMSC-3, CMSX-6, AMI...).

3.1.5 Alloy Properties

3.1.5.1 Solution heat treatment and recrystallization behaviour

Compared to CMSX-4, MC2 is more prone to recrystallization during the γ' solution heat treatment due to its lower value of γ' solvus temperature. Additions of Si and Hf in the MC2 modified alloy increase the γ' solvus temperature and then render the alloy less prone to recrystallization. For production of MC2 single crystal blades, the solution heat treatment temperature must be limited to 1290°C in order to avoid recrystallization.

3.1.5.2 Physical Properties

The density of MC2 is 8.62 compared to 8.70 g.cm⁻³ for the rhenium-containing alloy CMSX-4. Both alloys are comparable regarding thermal expansion and elastic compliance.

3.1.5.3 Mechanical Properties

Creep tests showed no significant differences between MC2 and MC2 + Si + Hf. At 850°C, MC2 did not attain the creep life of CMSX-4, but at 1050°C the creep strength of MC2 was significantly superior to that of CMSX-4 (fig. 2). At 980°C, both alloys were comparable.

As the high cycle fatigue (H. C. F.) life is controlled by the crack initiation mechanism on pores and therefore depends on the pore size, the I-I. C.F. tests performed at 600 and 950°C on MC2 and CMSX-4 single crystals cast by the same foundry process resulted in comparable lives. Load controlled low cycle fatigue (L. C. F.) at 600°C of notched and unnotched test bars showed no difference between MC2 and CMSX-4. Strain controlled L.C. F. tests at 1000°C and thermal fatigue tests of coated and uncoated blades at 1000 and 1150°C resulted in comparable lives with a slight advantage for CMSX-4.

3.1.5.4 Oxidation Resistance

Comparative cyclic oxidation tests were carried out at 1100 and 1150°C on bare MC2 and MC2 + PWA73 coating (fig. 3). The coated MC2 test bar met the required oxidation resistance. The bare material showed a poor oxidation resistance compared to CMSX-4, but additions of Si and Hf improved significantly the oxidation resistance without reaching the oxidation properties of CMSX-4.

3.1.5.6 Service Performance

Long term exposure annealing at 1050 °C for 200 hours did not confirm the expected formation of μ phase. There was no loss of ductility of preaged creep and impact specimens. Application of an aluminised coating on test bars and blades was feasible without any problems. Additional heat treatments (i.e. brazing) reduced equally the creep properties of both MC2 and CMSX-4.

The influence of thermomechanical damage on the creep behaviour of bare and coated material was evaluated. Two kinds of protective coatings were used on MC2 specimens: i) a PdNi modified alumina coating and ii) a NiCoCrAlYTaNi low pressure plasma spray coating. All creep tests were conducted at 1050°C and 140 MPa. On bare specimens, a small decrease of the creep life was observed during a preliminary thermal cycle at 1100°C for 8 hours, whereas some improvement of the creep life was obtained after a pre-treatment at 1100°C 8 hours under 140 MPa.

The MC2 specimens coated with a PdNi modified aluminide exhibited shorter creep life than bare material when pre-damaged at 1100°C for 8 hours (fig. 4). On the other hand, the MC2 specimens coated with NiCoCrAlYTaNi and pre-damaged at 1100°C for 8 hours under 140 MPa showed creep rupture life comparable to that of undamaged bare material. These results demonstrated the high microstructural stability of the alloy and the excellent behaviour at high temperature of the MC2/NiCoCrAlYTaNi combination.

3.2 Casting process development

3.2.1 Introduction

After a long period of single crystal technology development the so-called withdrawal process was successfully introduced into production. This process allows adjustment of the relevant parameters by heating devices, cooling baffles and a mechanical withdrawal unit. This piece of equipment is significantly more costly than a furnace for conventional equiaxed investment casting. It also dramatically increases the time for production cycles.

In a joint effort by some European companies it has been shown that, in principle, conventional furnaces are suitable for DS and SC production without any need of additional heating, baffle cooling and withdrawal devices. This approach, the SMCT-process, again shows a significant cost saving potential. Figure 5 shows the SMCT process in comparison to the conventional withdrawal process.

3.2.2 Process adaption

To prove the validity of the SMCT process for actual engine components two hollow high pressure turbine blades of complex cooling configuration were chosen, one to be cast by THYSSEN in CMSX-6 and the other to be cast by PRECICAST in MC2.

THYSSEN and PRECICAST were using molds with 20 blades per mold. Several molds were cast.

In conclusion the feasibility of the SMCT casting process could be proved for these components, but could not be transferred to an economic industrial scale during the project time due to difficulty in transferring the laboratory know-how to the production environment.

3.2.3 Improvement of casting process with regard to economical aspects

Costs for castings are mainly influenced by the yield of the process, the number of parts per cluster, the alloy quantity and the insulation.

The yield of this casting process was optimized with regard to recrystallisation, grain structure, secondary dendrites and gating system. For increasing the number of parts per mold, the blade spacing was reduced to accommodate 22 instead of 12 blades per mold. As the heat flux in this process is not dictated by external heating as in the conventional withdrawal process the number of parts can be increased by using a rectangular gating system.

To reduce the alloy quantity several molds with different heat reservoirs were made. The alloy quantity could be reduced to about 50 % without any influence on the quality of the castings,

Several insulation materials have been tested with regard to insulation property, handling, reusability and costs.

Insulation with hollow spheres gave the best results concerning all aspects (figure 6).

3.2.4 Process modelling /6/

Inverse modelling

The goal of inverse modelling is to combine numerical simulation tools with measurements to determine unknown quantities.

The principle of inverse modelling is to switch one input with the output.

This means thermal history as input is used to obtain either the boundary conditions, i.e. heat flux, heat transfer coefficient, emissivity or thermophysical properties, i.e. specific heat, thermal conductivity, latent heat. Within the framework of this project, inverse modelling was used to determine the diffusivity of CMSX-6 and to determine the heat flux at the chill-casting interface.

Modelling of a single blade

To develop, validate and apply a simulation tool to the modelling of the casting process, the following steps were achieved. The 3-D version of the simulation software was further developed. Castings of dummy and real blades were made (figure 6, 7). The appropriate properties and boundary conditions were defined in order to have good agreement between the measurements and the calculated cooling curves. The effects of the main process parameters were studied.

A new method to account for radiation was developed within the framework of this project. This method is called the "net radiation method", to account for grey body radiation. [It includes the automatic calculation of viewing factors with shadowing effects.

Modelling of a cluster

The case of a rectangular cluster was chosen (figure 8). The results are:

The solidification time is lowered by more than 1/3 if a smaller heat reservoir is used. Lower initial temperatures of the mold and of the insulation do not have a significant effect on the solidification time. If the insulation has a lower thermal conductivity (5 times smaller), the solidification times are doubled or more.

An improved insulation is favorable, as the gradient is larger and the G/v ratio is high enough to avoid a coarse microstructure. However the solidification time is about doubled, which means that the vacuum furnace will be occupied for a longer period of time.

3.3 Non Destructive Testing Method

3.3.1 Introduction

The availability of affordable and reliable single crystal components for high temperature applications, in particular in gas turbines, is nowadays an essential requirement for competitive engines. Due to the fact that any defect or disorientation of their crystal structure could have a significant influence on their in-service performances (creep, strength, . . .). these nickel base superalloy parts need additional non destructive investigations designed to determine the orientation of the crystallographic axes and, at the same time, reveal possible grain structure defects,

For the purpose, two non-destructive testing methods have been deeply investigated and are presented hereafter: the first one, called "CRISTAL" (Acronym for "Contrôle Radiocristallographique Industrial par Surveillance Topographique et Analyse de Lignes) is now in use at TURBOMECA on a production line, while the second one, called "REFOCALISATION", is still under development.

Both methods are based on high energy X-ray diffraction measurements. Conversely to the LAUE technique, these two NDT methods under study are not sensitive to oxydation/corrosion, protection coatings, residual stresses and surface imperfections (roughness, ..). They permit volume inspection of the whole part (blades or specimens) in terms of crystal quality and orientation as well as in terms of subgrain and defect. On the contrary, using LAUE measurement, only one crystal orientation assessment is possible and only on a very localized and small external area which is not always representative of the whole blade.

Additionally, both methods require an apparatus similar to that used for X-ray inspection: a fine focus high voltage X-ray generator and an X-ray intensifier coupled with a camera. Finally, they increase the reliability of quality inspection and are different as well as complementary, which will be explained in this report.

In parallel and in reply to the three objectives mentioned above, results on metallurgical, dimensional and N.D.T. investigations performed on pre-production quantities at and by TURBOMECA are presented hereafter. The TURBOMECA prototype, CRISTAL, was used to perform the radiocristallographic NDT investigations.

3.3.2 Method "CRISTAL"

3.3.2.1 Results in light of the CRISTAL technique

The principle of CRISTAL is shown on figure 3.1A.

The divergent beam, issued from the X-ray generator, illuminates the part under inspection placed a few centimeters from the focus. When the generator voltage is roughly above 80 kV, the emitted X-ray spectrum comprises two main constituents: first, the 2 characteristic rays of the Tungsten anode, $K\alpha$ (-58.5 keV) and $K\beta$ (-67.4 keV) and, second, the continuous "Bremsstrahlung" spectrum. The latter is bound on the low energy side by the absorption of the windows generator and on the high energy side by the value of the applied voltage.

In the observation plane, located a few decimeters away from the part, the diffracted and transmitted beams, both coming from two constituents (the characteristic rays and the continuous spectrum) are superimposed and can be evidenced and recorded. In this way, the image contrast is induced by the absorption and diffraction properties of the part. Black and white lines,

grouped by pairs, can then be observed and are superimposed on a strong continuous and nonuniform level signal (see figure 3.1 D).

The position and the orientation of these lines reflect the orientation of the crystal, while the defects of the grain structure are revealed by distorted or discontinuous lines. Figure 3.1 D evidences a disoriented subgrain and disorientation of the dendritic texture (also called mosaicity).

3.3.2.2 The computer simulation results

A computer program has been developed in order to simulate cross-sectional intensity profiles along any direction in the image plane and these simulations have been correlated with on-site experiments. Figure 1 B shows the intensity profile along the perpendicular of a (2,00) lattice plane calculated for a constant thickness crystal. It confirms that the lines observed on the recorded image are due to the characteristic $K\alpha$ and $K\beta$ radiations of the Tungsten and correspond to what has previously been called "Cossel lines" (7). Even if on one hand this method does not require a very high voltage generator (80-100 kV is sufficient), on the other hand, a very small focus size is recommended in order to obtain narrower diffraction lines. The simulation revealed also has limitations concerning the region of the part actually investigated since Bragg's condition is not fulfilled throughout the entire volume. Consequently, a complete inspection requires evolution of the position of the part. Finally and fortunately, even if CRISTAL is limited by the absorption of the characteristic rays, the thickness of TURBOMECA blade airfoils is in the range that this method can investigate. ‘

3.3.2.3 Assessments of crystal orientation: precision and computerized calculations and 3-D visualization

A campaign of crystallographic orientation measurements has been carried out on 30 Arrius IIC blades with both CRISTAL and the conventional technique LAÜE. LAUE serves as a reference in the foundry industries since it has been used for the last decade(s). Based on this comparison between the two techniques, CRISTAL is judged accurate and reliable.

Without any change of the mounting tool but only in the technique, the average difference between the two techniques is found to be only 0.15° with a standard deviation of $\pm 0.8^\circ$. Also, the reliability of the orientation measurement of CRISTAL and of LAÜE was found to be 0.3° and 0.65! respectively. Along these lines, the investigation zones between CRISTAL and LAUE are different: the airfoil for CRISTAL and the root for LAÜE.

Additionally, in order to visualize the orientation of the crystal within the single crystal cast blades and to facilitate interpretation of the castings and of the batch for the foundry, a computer simulation was performed (Service RDM de TURBOMECA). For each blade, three 3-D views can be obtained: a front, a side and a top view. For each view the crystal growth

axis and the respective perpendicular pole along which the X-ray investigation is performed can be shown.

3.3.2.4 The complete automation of CRISTAL

As a matter of fact, the major difficulty arises when considering the complete automation of CRISTAL. To the useful signal of the lines a ten times higher background signal strongly ununiform due to the absorption of the part is superimposed leading to images with a very weak contrast. Practically, this contrast, even more strongly heterogeneous for hollow blades, is responsible for preventing the automation of the inspection by this method.

In spite of these automation difficulties, it is important to recall that a visual and dynamical inspection conducted with CRISTAL by an operator has been developed. It remains a very easy method to implement and TURBOMECA routinely uses this method to inspect turbine blade airfoils thanks to its high quality assurance performances.

3.3.3 Method "REFOCALISATION" (8)

In order to try to overcome the limitations of CRISTAL, REFOCALISATION (8) has been investigated.

3.3.3.1 Results in light of the REFOCALISATION technique

This method is based on a peculiar white beam diffraction property' the principle of which is given in figure 3.2 A. For a given geometrical set-up layout, each volume of the single crystal part illuminated by the whole X-ray spectrum diffracts a peculiar wavelength according to Bragg's law. All these diffracted beams refocalize in a focal spot, symmetric to the generator focus with respect to the normal of the diffracting lattice planes.

Although the theory assumes a perfect line diffraction pattern for a perfectly punctual focus (figure 3.2 B), this so-obtained refocalization phenomena, taking place for a given lattice plane family, practically leads to linear spots in the focal plane.

Using the position and the orientation of these spots the calculations of the crystallographic orientation axes of the part can then be performed. Furthermore, as shown on figure 3.2 D, the grain structure defects are evidenced either by a broadening of these spots for mosaic crystal or by their splitting in the case of disoriented subgrains.

3.3.3.2 The computer simulation results

As for CRISTAL, cross-sectional intensity profiles in the focal plane have been calculated by simulation. Figure 3.2 C shows the one for the (2,0,0) reflection. Both diffracted beams originating from the characteristic rays and from the continuous spectrum are separated from the transmitted ones and are refocused together, within the focal plane, in a small spot. As a major

consequence, the useful signal has a high intensity and is not mixed with or superimposed on any other transmitted constituents, Al-so, with increasing voltage, the continuous spectrum can be extended on the high energy side and, by simply adjusting the voltage of the generator to compensate for the absorption effect, thicker parts can be investigated. Experiments have been successfully performed at 400 kV on samples up to 15 mm thick (figure 3.2 D). Finally, it is worth noting that for a well chosen geometrical set-up layout, the complete volume of the specimen can be inspected in one measurement and additionally the sensitivity and angular resolution can be adjusted and adapted to the study by modifying the distance L of the figure 3.2 A.

3.3.3.3 Complete automation of REFOCALISATION

Consequently and due to the fact that the heterogeneous absorption phenomena, which occur only along the transmitted beams, are eliminated and then do not perturb the diffraction pattern background, the image contrast is drastically improved, thus most likely allowing automatic analysis and diagnosis. This advantage over CR ISTAL is even more interesting when an inspection of *highly* complicated hollow parts is intended. However, when the disorientation of the crystal is large, interpretation of REFOCALISATION diagrams can become more difficult than with CRISTAL diagrams. In that case, the interpretation of the diagram may need, for an automatic diagnosis and analysis, the help of a computer simulation program.

3.3.4 Combination of CRISTAL and REFOCALISATION

Finally, as both methods use similar apparatus, the solution appears to be to associate CRISTAL and REFOCALISATION in the same inspection set-up in order to combine their complementary advantages. This combination should allow complementary and different image patterns to be obtained to facilitate automatic diagrams.

4 Conclusions

As far as the creep strength is concerned, the chemistry of the alloy MC2 which was defined previously by ON ERA is considered to be optimized. This alloy exhibits a castability comparable to that of competitive single crystal superalloys as demonstrated by casting trials performed using two different directional solidification processes. The microstructural features of the single crystal bars and blades cast by the two processes are similar to that obtained with other single crystal superalloy, The main advantage of MC2 is its creep strength in the temperature range 1000-1100 °C, which is superior to that of any other competitive single crystal superalloy including the recently developed rhenium containing alloys such as CMSX-4. This result has been obtained with a homogeneous and stable microstructure, by using a simple heat treatment procedure and by avoiding the addition of rare, heavy and expensive elements such as rhenium. The disadvantage of MC2 compared to CMSX-4 concerning the high temperature oxidation resistance can be partially eliminated by simultaneous additions of silicon and

hafnium, which improve the adherence of the protective alumina scale without influencing the creep behaviour. MC2 is more prone to recrystallisation than CMSX-4, but this disadvantage can be suppressed by decreasing the homogenization treatment temperature from 1300 to 1290 °C without changing the overall behaviour of the alloy.

As far as the SMCT casting process is concerned the process could be shown to be suitable for the single crystal solidification of turbine blades without the need for significant investment in specially dedicated equipment. On the other hand it turned out that the know-how transfer from laboratory people to production people requires a strong commitment to be successful. A modelling tool has been developed successfully which allows process variables to be optimized numerically rather than by casting trials. This is thought to be a remarkable progress in terms of reducing lead time and cost.

As far as a complete NDT investigation and diagnosis of single crystals is concerned, two radiocrystallographic non-destructive testing methods have been deeply investigated: "CRISTAL" and "REFOCALISATION".

In both cases, computer simulations have been obtained and physical phenomena have been understood in details which permit optimized experiments.

CRISTAL has been demonstrated as being a reliable NDT method to measure crystal disorientation with accuracy, and 3-D views showing how the crystal has grown within the component were obtained.

Because of the respective ability of both methods to permit volumina investigation of crystallographic orientations, imperfections and disoriented subgrains within the whole volume of the inspected part, the reliability of the quality inspection of the new generation single crystal components is significantly improved. These key advantages lead to an even more promising future when considering the inspection of the in-service components that usually undergo surface alterations during their life time since both methods are insensitive to surface and/or preparation.

For both methods, an image data base was generated and image treatment feasibility studies have been conducted.

The difficulty of extracting enough signal in the noise for "CRISTAL" or the complexity of the images for "REFOCALISATION" did not allow any image treatment methodology to achieve a 100% automated inspection, detection and diagnosis of the single crystal engine components.

As already said, since both methods use similar apparatus, the solution appears to be associating CRISTAL and REFOCALISATION in the same inspection set-up in order to combine their complementary advantages.

5 **References**

- [1] P. Caron and T. Khan, "Development of a New Nickel Based Single Crystal Turbine Blade Alloy for Very High Temperatures", *Advanced Materials and Processes*, Vol. 1: *Advanced Processing and High Temperature Materials*, edited by H.E. Exner et V. Schumacher, DGM Informationsgesellschaft mbH, Oberursel, RFA (1990) pp. 333-338

- [2] K. Harris, G.L. Erickson, S.L. Sikkenga, W.D. Brentnall, J.M. Aurrecoechea, K.G. Kubarych, "Development of the Rhenium Containing Superalloy CMSX-4 and CM 186 LC for Single Crystal Blade and Directionally Solidified Vane Applications in Advanced Turbine Engines", *Superalloys 1992*, edited by S.D. Antolovich et al., TMS, Warrendale, PA, USA (1992) pp. 297-306

- [3] P. Caron, S. Navéos and T. Khan: "improvement of the cyclic-oxidation behaviour of uncoated nickel based single crystal superalloys", *Conference on: Materials for Advanced Power Engineering 1994, Part II, Liege, Belgique*, edited by D. Coutsouradis et al., Kluwer Academic Publishers, Dordrecht, Hollande (1994) pp. 1185-1194

- [4] R.V. Mc Vay, P. Williams, G.H. Meier, F.S. Pettit, J.L. Smialek, "Oxidation of Low Sulfur Single Crystal Nickel-Base Superalloy", *SUPERALLOYS 1992*, edited by S.D. Antolovich et al., The Minerals, Metals & Materials Society, Warrendale, PA, USA, (1992) pp. 807-816

- [5] I.M. Allam, D.P. Whittle, J. Stringer, "The Oxidation Behaviour of CoCrAl Systems Containing Active Element Additions", *Oxidation of Metals*, 12, 1 (1978) pp. 35-66

- [6] Calcom-Bericht, CALCOM "Numerical Modelling of the SMCT-Process"
Final Report October 1994

- [7] Geisler, A. I-t., Hill J.K., & Newkirk J. B., "Divergent Beam X-ray Photography with Standard Diffraction Equipment", *J. Applied Physics*, 19 [1 1], pp. 1041-9 (1994)

- [8] Patents: France n°90/13330, Europe n°91.420373 .2, USAA n°07/779191

6 **Acknowledgments**

The project was supported by the European Community under the title "Economic and Reliable Turbine Blading by Low Cost Single Crystal Alloy, Casting Process and Non Destructive Testing.

Contract No.: BREU-0422,
project No.: BE-4515

Table I : Chemical analyses of the MC2 and MC2 modified nickel-based superalloys (wt.%)

Element	Co	Cr	Mn	W	Al	Ti	Ta	C (ppm)	S (ppm)	Si (ppm)	N (ppm)	Ag (ppm)	Ri (ppm)	Ph (ppm)
MC2 (nominal)	5	8	8	8	8	8	5	1.5	6					
MC2 VM 1913	5.08	7.86	2.07	7.85	4.87	1.53	6.05	20	10					
EX 51	5.17	7.99		2.12				8.12	4.89	200	1.21	5	10	<2
FC 38	4.97	8.1		1.98		7.25		4.96			1.46	6		
FY 88	6.01			2.03		8.04		4.9		1.53	5.86			
FZ 88	8.06	3.00	6.04	5.56		7.17								
FZ 91	7.97	1.5	8.00	5.50		6.70								

Table II : Creep data on MC2 and MC2 modified fully heat-treated <001> single crystals

Alloy	Temperature (°C)	Stress (MPa)	Time for 1% creep (h)	Time to rupture (h)	Elongation to rupture (%)
MC2	760	750	504	1 972	10.3
	850	500	190	621	15.0
	950	240	200	637	16.0
	1000	200	300	604	11.4
	1010	170	772	1057	10.4
	1050	145		804	5.5
	1050	140	631	896	5.8
	1100	130	254	292	
EX51	850	500	139	750	>11.8
	950	240	195	585	27.2
	1000	200	81	268	19.2
	1050	145	269	357	12.0
FC 38	850	500	111	425	19.9
	950	240	137	553	24.6
	1000	200	63	283	1.6
	1050	145	521	626	4.6
FY 88	760	750	42	394	10.5
	850	500	54	305	18.9
	950	240	96	449	37.6
	1000	200	58	183	14.6
	1010	170	14.4	373	16.8
	1050	140	321	431	18.2
FZ 88	760	750	65	353	12.6
	850	500	46	220	23.4
	950	240	86	314	28.9
	1050	140	247	401	7.9
	1100	130	43	61	10.3
FZ 91	760	750	73	388	9.6
	850	500	71	269	12.7
	950	240	126	393	23.3
	1050	140	208	291	10.8
	1100	130	16	58	9.8
MC2+Si+Hf	760	750	175	930	8.6
			336	1 147	5.3
	850	500	139	447	12.6
	950	240	195	530	13.4
			140	391	24.0
	1010	170	330	561	8.1
			282	547	20.3
	1050	140		1 006	11.2
			934	5.9	

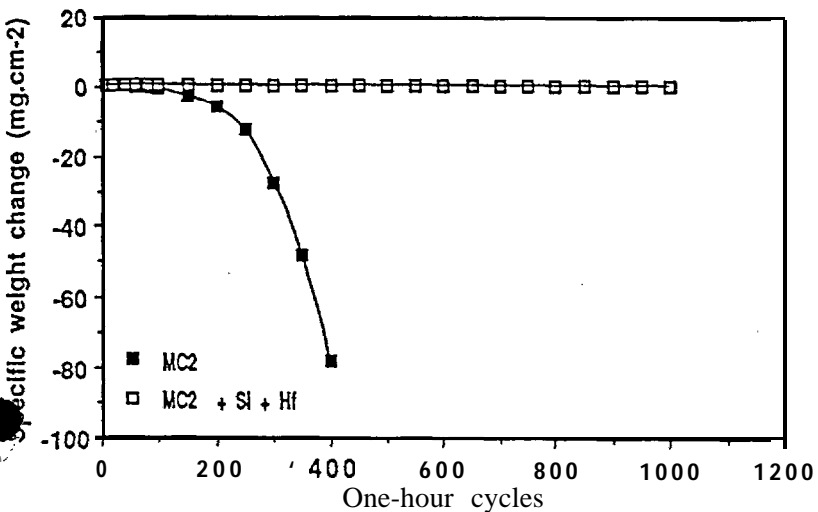


Figure 1- Cyclic oxidation behaviour in air at 1100°C of fully heat-treated MC2 single crystal alloys,

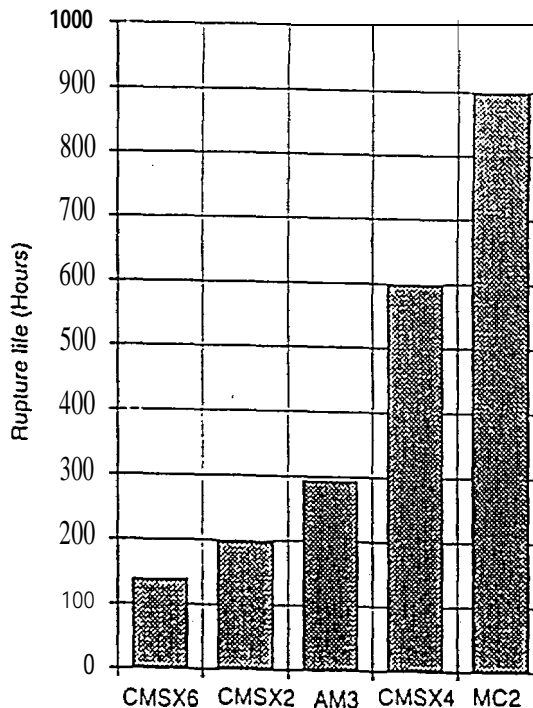


Figure 2- Creep rupture life at 1050°C and 140 MPa of various single crystal superalloys.

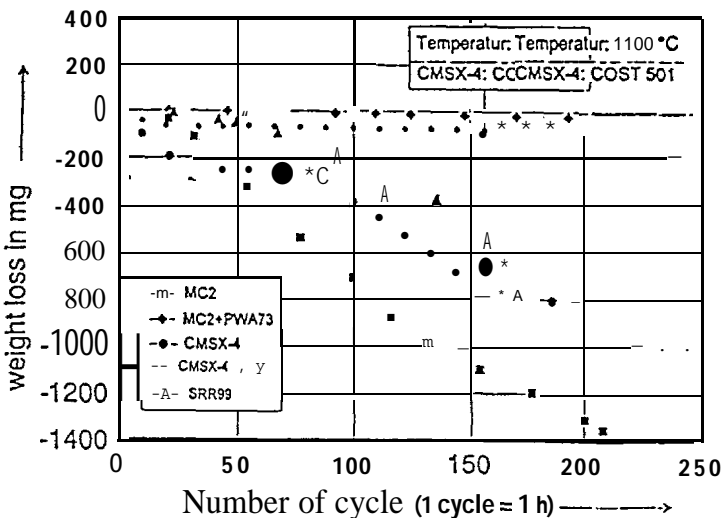


Figure 3- Cyclic oxidation behaviour of MC2 with and without coating.

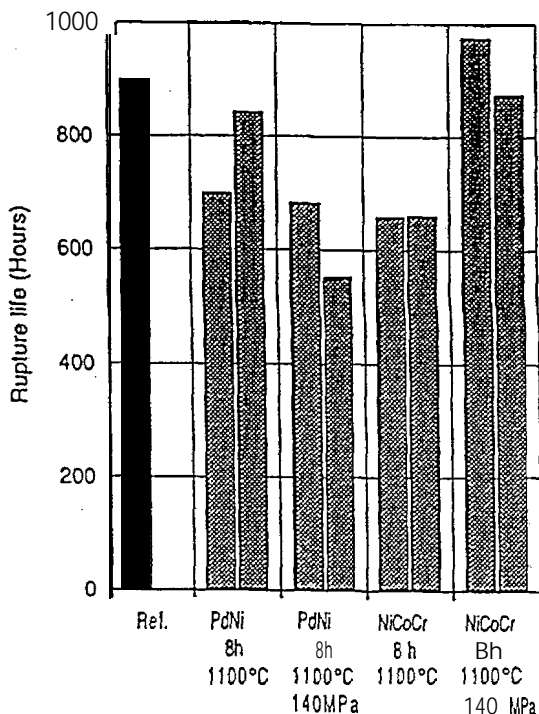


Figure 4- Pre-damage influence on creep life at 1050°C and 140 MPa of coated MC2.

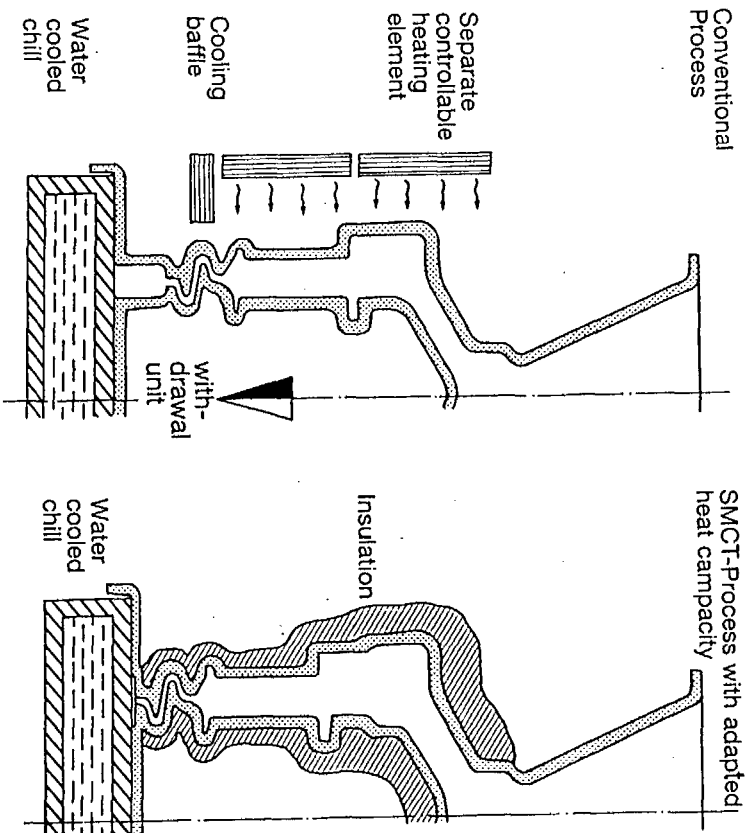


Figure 5: SMCT-process in comparison to the conventional process

Testing of insulation materials

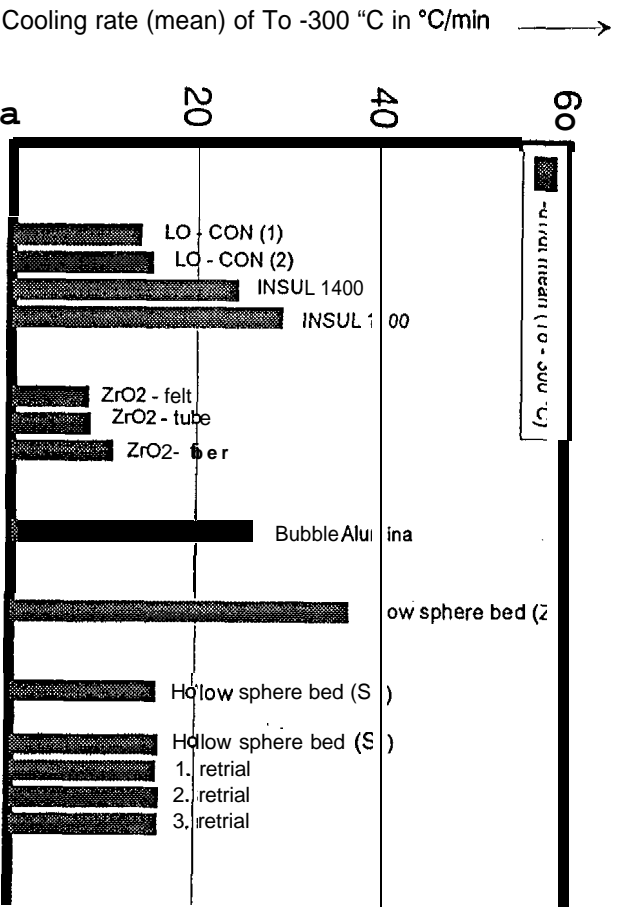


Figure 6: Testing of insulation materials

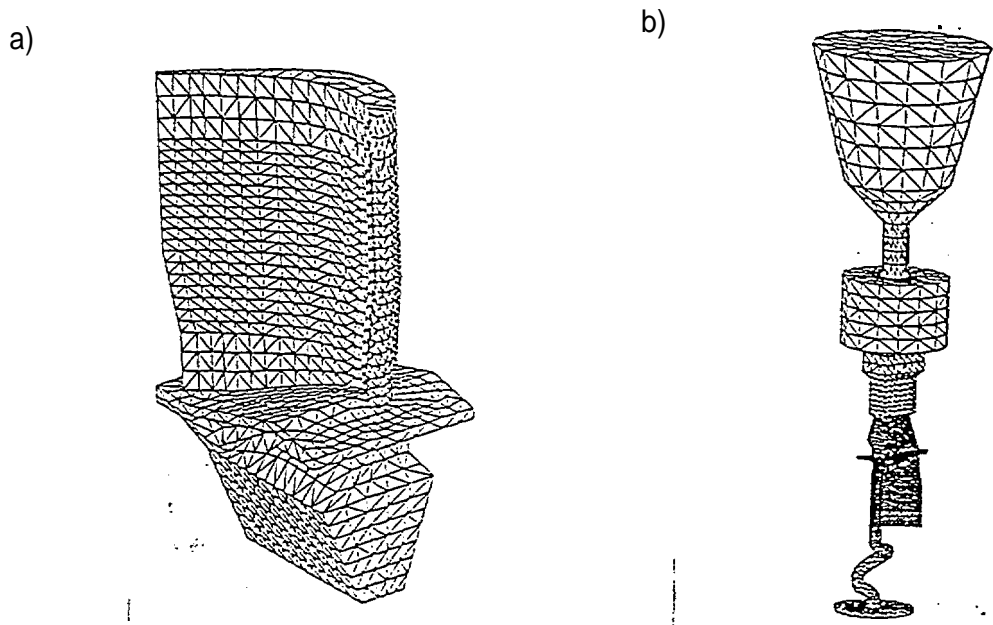


Figure 7: Surface mesh of a real blade a) blade b) whole casting

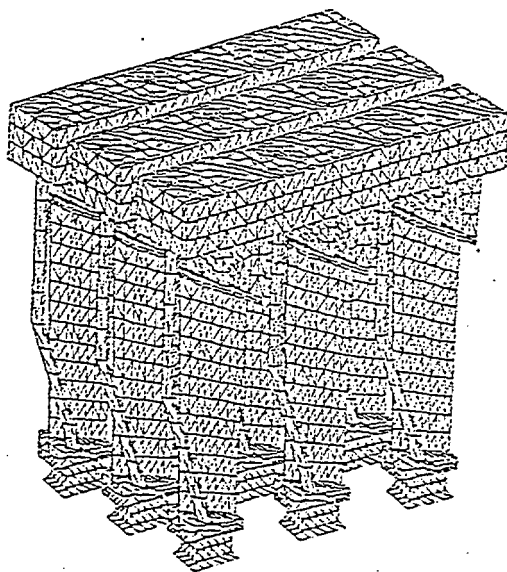
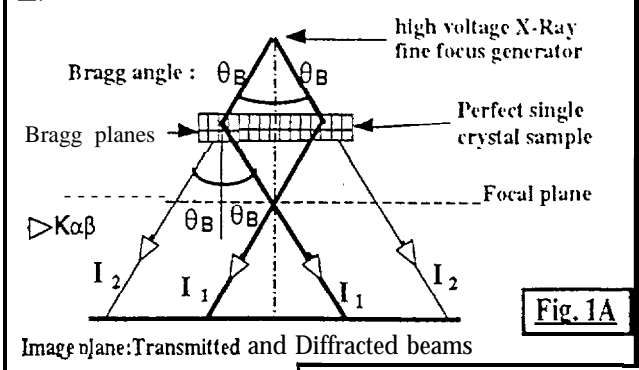
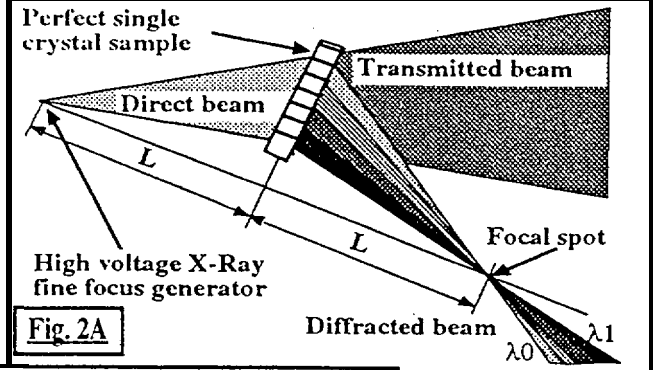


Figure 8: Mesh of a rectangular cluster

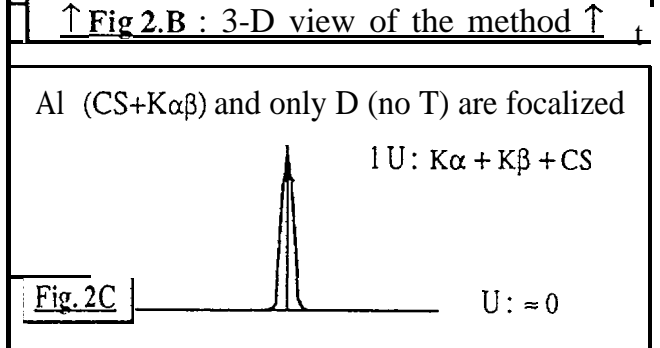
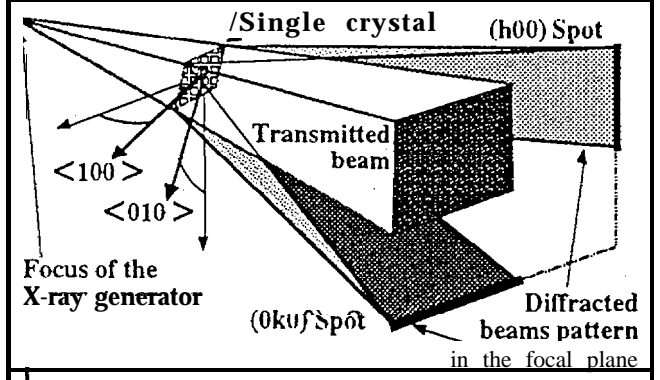
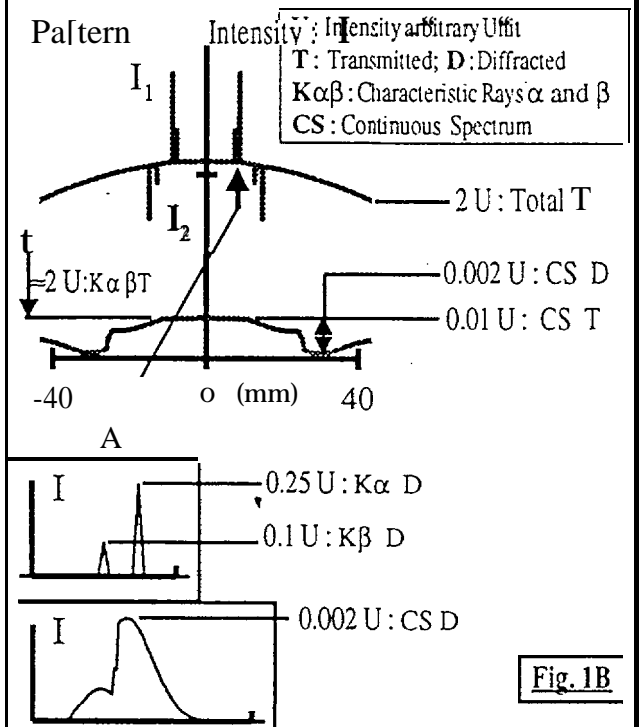
CRISTAL



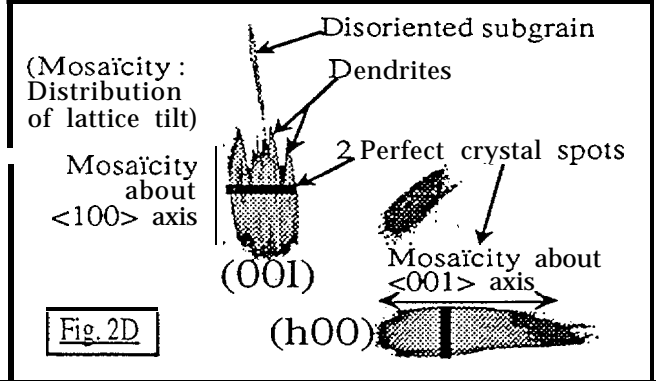
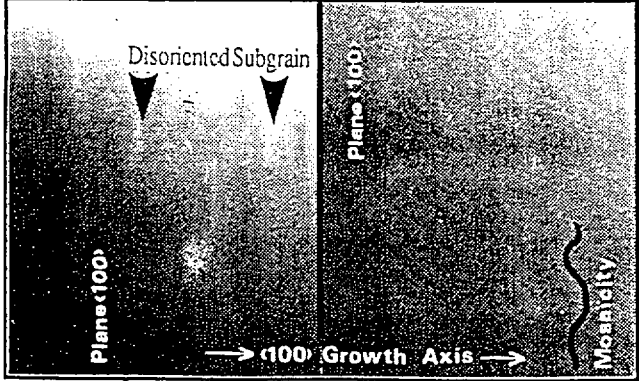
REFOCALISATION



↑ Fig 1A and 2A : basics of both methods ↑



↑ Fig 1B and 2C : Computer simulated diffraction pattern profiles for both methods ↑



↑ Fig 1 D and 2D : Experimentally recorded diffraction patterns ↑

Fig. 3.1 and Fig. 3.2

Principles of the methods investigated